Polymer 50 (2009) 3661–3669

Contents lists available at ScienceDirect

Polymer

journal homepage: www.elsevier.com/locate/polymer

Nanofibrous chitosan non-wovens for filtration applications

Keyur Desai [a], Kevin Kit [a,*], Jiajie Li [b], P. Michael Davidson [b], Svetlana Zivanovic [b], Harry Meyer [c]

[a] Department of Material Science and Engineering, University of Tennessee, Knoxville, TN 37996, USA
[b] Department of Food Science and Technology, University of Tennessee, Knoxville, TN 37996, USA
[c] HTML Share user facility, Oak Ridge National Laboratory, Oak Ridge, TN 37831, USA

ARTICLE INFO

Article history:
Received 8 April 2009
Received in revised form
12 May 2009
Accepted 19 May 2009
Available online 6 June 2009

Keywords:
Chitosan
Filtration
Nanofibers

ABSTRACT

Chitosan containing nanofibrous filter media has the advantage of filtering material based on both its size and functionality. They can be potentially applicable in a wide variety of filtration applications ranging from water purification media to air filter media. We have fabricated nanofibrous filter media by electrospinning of chitosan/PEO blend solutions onto a spunbonded non-woven polypropylene substrate. Filter media with varying fiber diameter and filter basis weight were obtained. Heavy metal binding, anti-microbial and physical filtrations efficiencies of these chitosan based filter media were studied and correlated with the surface chemistry and physical characteristics of these nanofibrous filter media. Filtration efficiency of the nanofiber mats was strongly related to the size of the fibers and its surface chitosan content. Hexavalent chromium binding capacities up to 35 mg chromium/g chitosan were exhibited by chitosan based nanofibrous filter media along with a 2–3 log reduction in *Escherichia coli* bacteria cfu.

1. Introduction

There is an enormous requirement for cleaner air and water around the world which has sparked immense interest in the development of high efficiency filters. Fibrous media in the form of non-wovens have been widely used for filtration applications. Non-woven filters are made of randomly laid micron-sized fibers which provide a physical, sized-based separation mechanism for the filtration of air and water borne contaminants [1]. Non-woven nanofibrous filter media (nanofiber is defined as having diameter <0.5 μm by non-wovens industry [2]) would offer a unique advantage as they have high specific surface area, good interconnectivity of pores, and ease of incorporation of specific functionality on the surface effectively filtering out contaminants by both physical and chemical mechanisms. A number of companies are developing nanofibrous filter media such as Donaldson Company (Ultra-Web and Fibra-Web), Finetex Mats™, Amisol EA Air Filters [2].

Chitosan, a polycation, is a non-toxic, biodegradable polysaccharide which can derived from naturally occurring chitin. Chitin is the second most abundant polysaccharide found in the exoskeleton of crustaceans, crab and shrimp shells, insects and fungal mycelia [3,4]. Chitinous biopolymers have also been found in wastes of mushrooms such as *Agaricus bisporus* (most consumed variety of mushroom in the US) [5]. Based on the mushroom waste generated annually, mushrooms could yield up to 1000 metric tons of crude fungal chitin. Chitosan is a copolymer of *N*-acetyl-D-glucosamine and D-glucosamine, and the D-glucosamine content is dependent on the degree of deacetylation (DDA) of chitin to chitosan. Chitosan has a pK_a near 6.5 and in slightly acidic solutions, some of the amine groups become protonated [6]. The fraction of repeat units which are positively charged is a function of the degree of deacetylation and solution pH. A higher degree of deacetylation would lead to a larger number of positively charged groups on the chitosan backbone. Sorlier et al. [6] have studied the effect of pH and degree of deacetylation (DDA) on chitosan solution pK_a and found that for varying DDA from 5% to 75%, pK_a varies between 6.3 and 7.2. Chitosan has several unique properties such as the ability to chelate ions from solution and to inhibit the growth of a wide variety of fungi, yeasts and bacteria [7]. The antibacterial properties of chitosan are due to the interaction between the positively charged amine groups on the chitosan backbone and negatively charged components in the microbial cell membranes. Binding between chitosan and cell wall components alters the barrier properties and prevents entry of nutrients or causes leakage of intracellular components [8], both of which lead to death of the cell. The factors that affect the antimicrobial effectiveness of chitosan are similar to those that affect its metal binding capacity like degree of deacetylation, pH, molecular weight, crystallinity, and microbial buffer solution temperature [9].

Electrospinning is a process by which sub-micron sized polymer fibers can be produced using an electrostatically driven jet of

* Corresponding author. Tel.: +1 865 974 7055; fax: +1 865 974 4115.
E-mail address: kkit@utk.edu (K. Kit).

0032-3861/$ – see front matter © 2009 Elsevier Ltd. All rights reserved.
doi:10.1016/j.polymer.2009.05.058

polymer solution [10]. The fibers are collected as a non-woven mat. Electrospun nanofiber mats offer a distinctly high surface area to mass ratio (typically ranging from 40 to 100 m^2/g, compared to 0.05–10 m^2/g for micron sized spunbonded or melt blown non-wovens) which can be beneficial in a variety of applications. Using electrospinning to fabricate nanofibrous filter media, the fiber diameter, filter thickness and porosity can be controlled. The total available active surface area of nanofibrous filter media is directly proportional to mass of the fiber mat and inversely proportional to fiber diameter. The present use of nanofibrous filter media is limited to pre-filtration, due to its small pore size and lack of self-supporting mechanical strength [1]. Nanofibrous filter media have been fabricated and tested by electrospinning a layer of synthetic polymer fibers of nylon-6, polyvinylidene fluoride, and polyacrylonitrile onto melt blown or spunbonded non-woven substrates for varied applications such as for aerosol particulate filtering [11,12], high efficiency particulate air filters (HEPA) [13], antimicrobial air filter [14,15], coalescence oil filter [16] and catalytic filters for recycling and reusing highly specific catalysts like enzymes [12]. All these studies showed that addition of the nanofibrous layer increased the filtration efficiency with slight increase in pressure drop. The improvement in performance is due to physical characteristics of the nanofibrous layer i.e. small fiber size and small filter pore size. Chitosan based nanofibrous filter media would offer a unique advantage of using both physical and chemical mechanisms to effectively neutralize toxic pollutants from air and liquid media, delivering the next generation of non-toxic, environmentally benign filter media made from naturally occurring biodegradable materials.

We have previously reported the fabrication of chitosan/PEO nanofibers made using 90% chitosan in blend solution with fiber diameters as low as 80 nm [17]. Fiber formation improved with addition of PEO and beadless nanofibers were obtained by addition of 25% PEO in blend solutions. These nanofibers, when tested for their metal binding efficiencies, showed high binding capacities up to 16 mg chromium/g chitosan [17]. In the current work, nanofibrous filter media have been fabricated by electrospinning chitosan:PEO (90:10) blend solutions onto a spunbonded polypropylene (PP) substrate, and nanofibrous filter media with varying fiber diameter and basis weight (thickness of nanofiber layer) were obtained. To characterize the filtration efficiencies of these nanofibrous filter media, a dynamic filtration unit was set up which could simulate a real-time filtration environment and the Cr(VI) bonding, anti-microbial and physical (polystyrene bead and aerosol) filtration efficiencies of the nanofibrous filter media were tested. This is the first comprehensive study which demonstrates the applicability of chitosan based nanofibrous filter media for air and water filtration.

2. Materials and methods

2.1. Materials

Chitosan with two different molecular weights was used. Chitosan of molecular weight Mw = 1400 kDa (HMW) with varying degree of deactylation (DDA) i.e. 80%, 70%, and 67% DDA was used as-received from Primex Inc. Chitosan of lower molecular weight Mw = 100 kDa (LMW) and 83% DDA was used as-received from Sigma. Polyethylene oxide (Mw = 900 kDa) was used as-received from Scientific Polymer Inc. The solvent for making electrospinning solutions, acetic acid (AA) was purchased from Sigma.

2.2. Fabrication of nanofibrous filter media

The nanofibrous filter media was fabricated by electrospinning the chitosan solutions directly onto a 36.5 gsm (g/m^2) spunbonded polypropylene (PP) mat obtained from The University of Tennessee Non-wovens Research Lab (UTNRL). The electrospinning apparatus consisted of a metered flow pump (Harvard Apparatus Pump II), and a high DC voltage supply (Gamma High Voltage Research, Inc. Model HV ES 30P/DAM). The solution was ejected through a syringe (Popper & Sons,7935) using a feed rate of 0.08 ml/min, an applied voltage of 30 kV, and tip-target distance of 10 cm. Electrospinning solutions were prepared by dissolving the required polymers on wt% basis in the solvent and stirring the solutions for 24 h to make a well mixed homogenous solution. Circular discs of 47 mm diameter were cut from these composite fibrous media for characterization of metal binding, anti-microbial filtration and polystyrene particle filtration efficiencies. For measuring aerosol filtration efficiency, a 178 mm square mat was cut.

2.3. Filter media structural characterization

The nanofibrous filter media were characterized using field emission scanning electron microscope (FESEM, LEO 1525) to study the fiber morphology. The SEM samples were sputter coated with gold to prevent charging during SEM imaging. Image processing software ImageJ (NIH) was used to measure the fiber diameter from the SEM micrographs. For each sample, fiber diameter was measured at 60 different points. The basis weight (g/m^2 or gsm) of the nanofibrous filter media was measured using ASTM D 3776-96. It is measured by dividing the weight of a filter mat by its area. The porosity of the nanofibrous filter media was measured using a PMI capillary flow porometer (Porous Materials Inc.). A wetting liquid Galwick™ (Porous Materials Inc.) was used as a wetting liquid to spontaneously fill the pores in the nanofibrous membrane. The maximum pore size was detected as gas flow began through a wetted sample at bubble point pressure. The complete pore analysis was difficult to achieve as the nanofibrous mat delaminated from the spunbond PP substrate even at low pressure. The air permeability, which is another measure of the porosity of the nanofibrous membrane, was measured according to ASTM D737-96 using a Textest FX 3300.

2.4. Surface chemistry

The surface chemistry of the electrospun fibers was characterized using Thermo Scientific K-alpha X-ray photoelectron spectrophotometer (XPS) at the Shared Research Equipment (SHaRE) User Facility at the Oak Ridge National Laboratory. Monochromatic Al K-α X-rays (1480 eV) were used. A spot size of 400 microns (maximum allowable) was used to scan the surface of the samples so as to account for surface variations and obtain an averaged signal. A surface scan of the sample identified the chemical moieties on the sample surface, and a high resolution scan for "C", "N" and "O" was performed to identify the elemental peaks with varied chitosan % in blend fiber, chitosan DDA, fiber diameter, chitosan molecular weight, and after metal binding of blend fibers (average of 30 scans). XPS data was analyzed using Thermo Avantage V 3.74 software to calculate atom% of various elements found on electrospun fiber sample surface. Peak fitting was done on the high resolution elemental scans (average of 10 scans) to obtain surface chemistry information. To correct for the surface charging effect, the C1s electron binding energy was shifted to characteristic value 285.0 eV obtained from literature [18] and the flood gun was turned on.

2.5. Metal binding

The metal binding properties of the electrospun fiber mats were measured using the NIOSH manual of analytical methods (NMAM)

[19]. Chromium solution (5 mg/l) was made by diluting the standard 1 mg/ml K_2CrO_4 solution purchased from Sigma. The set-up consisted of a filtration flask, filtration funnel and a fritted glass filter support of 47 mm diameter. The filtration unit was used as-received from Millipore (Millipore 47 mm All-Glass Vacuum Filter Holder, XX15-04700). The composite fiber membranes fabricated as mentioned earlier were placed on top of the filter support and the assembly was clamped. Chromium solution (100 ml, 5 mg/l) was passed through the filter membrane for ten consecutive passes. A slight vacuum of ~1 mm Hg was applied to maintain a filtration time of 2 min. After each pass of 100 ml chromium solution, 1 ml of solution was removed from the sample and analyzed for chromium content. The latter was added to 7 ml of 0.5 N sulphuric acid (H_2SO_4). Diphenylcarbazide solution (0.5 ml) was added to above solution (as an indicator) and volume was adjusted to 25 ml by adding 0.5 N H_2SO_4. The chromium ion absorbance was measured at 540 nm using a Shimadzu UV–vis spectrophotometer (UV2102 PC, Shimadzu). Before each experiment, the spectrophotometer was calibrated and standard curves obtained by measuring absorbance for solutions prepared with known chromium concentrations (0–0.2 mg/L). For the nanofibrous filter mats, metal binding was determined by reading the chromium concentration at measured absorbance from the standard curves and then calculating the metal binding capacity on weight basis i.e. mg chromium/g chitosan. Measurements were done in triplicates.

2.6. Anti-microbial

The antimicrobial properties of the electrospun fiber mats were determined using *Escherichia coli* K-12, as the test microorganism. *E. coli* K-12 was grown in Brain Heart Infusion (BHI; Difco) broth for 48 h at 35 °C. Anti-microbial properties were tested under both static and dynamic conditions. For static testing, fiber mats of known weight were submerged into culture tubes containing 9 ml sterile phosphate buffer (0.05 M, pH = 7.08) inoculated with ca. 10^6 CFU/ml bacteria, and mixed by vortexing and incubating for 6 h at 25 °C. Phosphate buffer with the same *E. coli* K-12 inoculum but with no fiber was used as positive control and phosphate buffer with fiber but no inoculum as the negative control. The survival of *E. coli* K-12 was determined using the pour-plate method on Trypticase Soy Agar (TSA) medium [20]. All measurements were performed with 3 replications. The reduction in *E. coli* count was reported as log reduction which is defined as:

$$\log \text{reduction} = \log(\text{initial bacteria concentration}) - \log(\text{final bacteria concentration}).$$

The dynamic anti-microbial filtration properties were tested using the same Millipore unit described above. It was found that when 100 ml of 7 log concentration of *E. coli* K-12 test microorganism was passed through the filter membrane once it was overwhelmed by the high initial concentration of bacteria, and flow was completely blocked. Further tests were conducted by using a lower concentration of 4 log of *E. coli* K-12 test microorganism. The anti-microbial efficacy of the filter membrane was determined in the same manner as explained for the static test.

2.7. Polystyrene latex beads

The liquid filtration efficiency of the nanofibrous filter media was assessed by passing 10 ml of 200 ppm 3 μm diameter polystyrene latex beads (obtained from Sigma) using the Millipore filtration unit. The concentration of polystyrene latex beads in water was measured using a Shimadzu UV–vis spectrophotometer (UV2102 PC, Shimadzu) at 490 nm wavelength. Stock solutions of varying ppm of PS latex beads were prepared and a master curve of concentration vs. absorbance was obtained using the UV–vis. The concentration of the filtrate was interpolated from the known absorbance value obtained by UV–vis measurements of the filtrate solution. Measurements were done in replicates of three.

2.8. Aerosol filtration

The aerosol filtration efficiency was measured using a TSI Corp. model 8130 automated filtration testing unit at UTNRL. NaCl aerosol particles of 0.26 μm mean diameter, 0.075 μm count median diameter and concentration of 15–20 mg/m^3 were used. The penetration and pressure drop across the 178 mm square nanofibrous filter media was measured.

2.9. Statistical analysis

Various data collected for structural and filtration performance of nanofibrous filter were analyzed using the one-way Anova Tukey–Kramer test for statistical difference in means between different sample groups using the JMP 6.0 statistical analysis software.

3. Results and discussion

3.1. Fabrication of nanofibrous filter media

The goal of this research is to develop chitosan based nanofibrous filtration media which possess enhanced filtration efficiencies owing to the positive charge on filter fiber surface and size effect of nanofibers. As reported earlier, we were able to fabricate chitosan/PEO blend nanofibers in different size ranges and different blend ratios [17]. Nanofibers with higher chitosan % in blend solution (90%), higher molecular weight (HMW chitosan) and higher degree of deacetylation (80% DDA) exhibited the highest metal binding efficiencies for chitosan/PEO blend fibers [17].

A nanofibrous filter media comprising of a top layer of chitosan blend nanofibers electrospun on a spunbonded non-woven PP fiber substrate was fabricated. Spunbonded PP was used to provide mechanical and structural support to the thin layer of electrospun nanofibers. Initially melt-blown non-woven PP mats were chosen as the substrate as melt-blown mats have finer fibers and lower pore size compared to spunbonded non-wovens. However, it was not possible to electrospin a continuous layer of chitosan fibers on melt-blown PP webs, possibly due to the dense nature of the PP mat. Electrospinning of chitosan blend solutions on spunbonded PP substrates led to successful fabrication of chitosan based nanofibrous filter media. Filter media of HMW chitosan/PEO blends were fabricated with 90% chitosan in blend solution, while varying the electrospun mat density (achieved by spinning for different times), fiber diameter, and chitosan DDA.

To obtain varying fiber diameter HMW chitosan: PEO blends the strength of the acid solution was varied and a non-ionic surfactant Brij-35 (polyoxyethyleneglycol dodecyl ether) was used. Our collaborators at University of Massachusetts, Amherst, Kriegel et al. [21] have shown that increasing strength of acid reduces solution surface tension with an increase in solution viscosity and addition of 2 mM brij-35 leads to increase in solution viscosity with slight increase in solution conductivity and surface tension. Thicker fibers are formed by spinning 1.33 wt% HMW chitosan: PEO (90:10) blends with increasing strength of acetic acid from 75% to 90% and addition of 2 mM brij-35 as shown in Fig. 1. Fiber mats of different basis weight (0.5, 1 and 1.5 gsm) were fabricated by spinning for different times (1–4 h).

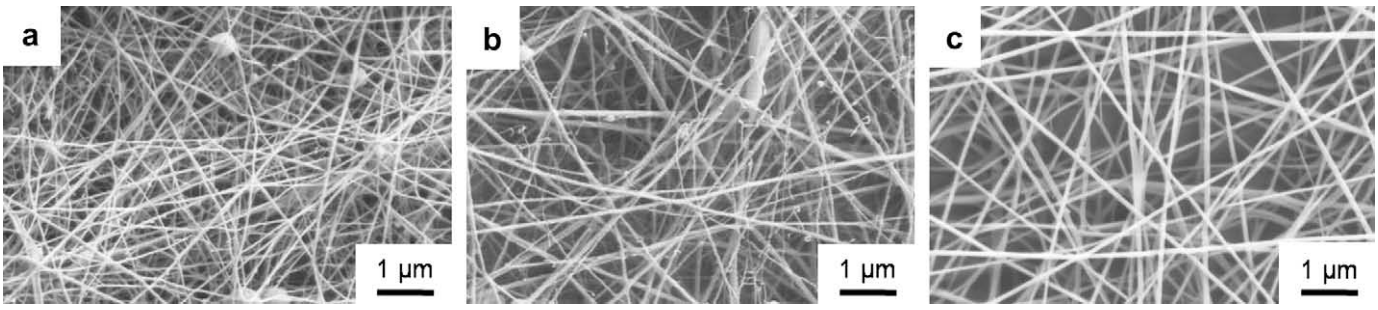

Fig. 1. SEM images and fiber diameter of 1.33 wt% HMW chitosan:PEO (90:10) fibers spun on spunbonded PP (a) using 75% acetic acid (fiber diameter = 88 (±24) nm), (b) using 90% acetic acid (fiber diameter = 114 (±37) nm), (c) using 75% acetic acid + 2 mM brij-35 (fiber diameter = 132 (±34) nm).

3.2. Surface chemistry of nanofibrous filter layer

X-ray photoelectron spectroscopy (XPS) analysis of surface of electrospun fiber mats was performed to determine the chitosan surface composition of the fiber blends. XPS scans of pure 80%DDA HMW chitosan films solvent cast from 1% HCl, and pure PEO solvent cast from water served as references (Table 1). Atomic % of the three main elemental peaks i.e. carbon, nitrogen and oxygen obtained from the XPS analysis of blend fibers was compared to those that can be derived theoretically knowing the chemical structure of the repeating unit of the individual polymers to calculate the weight fraction of chitosan present on fiber surface. It can be seen from the data in Table 1 that the surface elemental composition as obtained from XPS for the pure polymers is in close agreement with those obtained theoretically from the structure of their repeat units. The concentration of C1s peak is higher than the theoretical value and this could be due to surface contamination (similar results have been obtained for surface analysis of chitosan and PEO in literature [22–24]). Fig. 2 shows the "C", "N", and "O" elemental scans for the pure chitosan film. The elemental scans are in agreement with those obtained by Matienzo and Winnacker [22]. Peak fitting of the carbon curve shows presence of four different signals. The structure of chitosan is very complex, and Matienzo and Winnacker have correlated each of the four different carbon signals with structure of glucosamine and *N*-acetyl glucosamine units that make up chitosan. The carbons at C2, C6 from glucosamine along with the C2, C6, and C8 from *N*-acetyl glucosamine make up one carbon environment (30.08%, 285.0 eV) consisting of C–C or C–H linkages. The carbons at C3, C4 and C5 of both glucosamine and *N*-acetyl glucosamine make up a second carbon environment (51.37%, 286.66 eV) consisting of C–OH, C–O linkages. The carbons at C1 "O–C–O" makes up the third environment (16.32%, 288.25 eV) whereas the carbons at C7 (H_2N–C=O) in the *N*-acetyl glucosamine makes up the fourth environment (2.2%, 289.43 eV). The nitrogen curve also shows two peaks corresponding to the 58.48% protonated amine (400.3 eV) and 41.52% unprotonated amine (398.3 eV) [22]. The oxygen curve shows presence of three regions contributed by the carbonyl groups, ether linkage and hydroxyl groups present in chitosan. The elemental scans for PEO (Fig. 2) also show expected peaks. The C1s peak from PEO shows three different regions at 283.4, 284.97 and 287.22 eV. The peak at 284.97 and 287.22 eV can be attributed to the C–C, and C–O linkages present in PEO respectively. In insulating samples a small peak is seen at lower binding energies (~283 eV), and this is not attributed to any chemical group in the structure but to charging effects on the sample surface [25]. The O1s peak in PEO shows a single peak at 531.0 eV [24].

Fig. 3 shows a plot of the surface nitrogen composition (atom%) as obtained from XPS vs. the chitosan concentration (wt%) in solution. It can be seen that with decreasing chitosan content the atom% N (or surface content of chitosan) is decreasing. Also it can be seen that blend solutions made using higher molecular weight (HMW) chitosan have higher surface nitrogen content than low molecular weight chitosan blends for same blend ratios. As chitosan % in blend solution decreases, the elemental "C" peak of the blend fibers starts to lose its characteristic shape and evolves in to a broad peak which begins to narrow as concentration approaches that of pure PEO (which has a narrower C1s peak, Fig. 4) in blend solution. The N1s peak for pure chitosan shows two peaks but for the blend samples the protonated peak is not evident and the size of the protonated peak is decreasing (Fig. 4).

Table 1
Surface atomic composition of pure polymers obtained from their structure and XPS analysis.

Sample		Atom%				"C/N" ratio
		C1s	N1s	O1s	Cl2p	
80% DDA HMW	Theoretical	56.14	8.77	35.08		6.4
chitosan	From XPS (film)	61.11	5.6	28.18	5.11	10.92
Pure PEO	Theoretical	66.67		33.33		∞
	From XPS (film)	66.77		32.39	0.11	∞

3.3. Metal binding properties of nanofibrous filter media

3.3.1. Effect of fiber diameter and gsm

Our earlier work on Cr(VI) binding using chitosan/PEO blend fibers showed that binding decreased with increasing % PEO in blend solution and decreasing molecular weight of PEO [17]. XPS analysis of the blend fibers supports this result as we see that surface chitosan content decreases with increasing PEO in blend fibers and decreasing molecular weight of chitosan. As these chitosan/PEO blend fibers are intended for filtration applications, the Cr (VI) binding efficiencies of our nanofibrous mats were determined in simulated flow conditions as opposed to the static studies reported previously [17].

The dynamic metal binding properties of chitosan blend fiber mats were measured using the procedure described earlier. The pH of the prepared K_2CrO_4 solution was 7.3 and at that pH K_2CrO_4 dissociates into CrO_4^{-2} [26]. K_2CrO_4 (100 ml, 5 mg/l) solution was passed through chitosan nanofibrous filter media ten consecutive times and samples were taken after each pass to determine reduction in solution chromium concentration. It was seen that with each additional pass, the amount of binding increased. Therefore, for all tests on mg chromium bound per gram chitosan fiber are reported after the 5th and 10th passes.

All data showed herewith is for chitosan fibers made using HMW chitosan of 80% DDA except when otherwise noted. Fig. 5 shows the Cr (VI) binding capacity of HMW chitosan: PEO (90:10) blend fibers as a function of fiber diameter using 0.5 and 1 gsm chitosan nanofibers. It can be seen that with increasing fiber diameter, binding capacity decreases or remains statistically unchanged. It should be

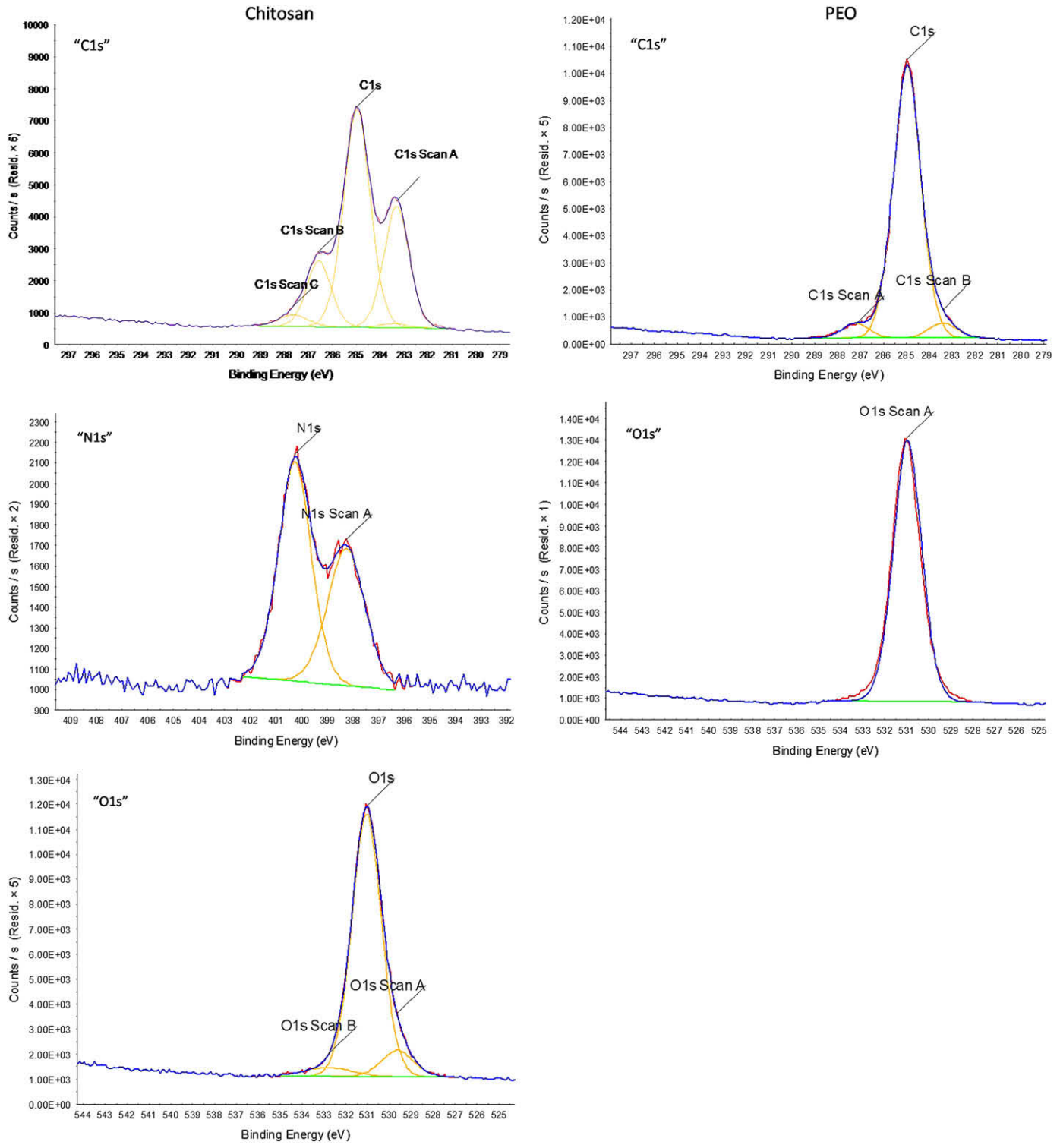

Fig. 2. High resolution "C", "N" and "O" elemental scans of pure chitosan(left) and high resolution "C" and "O" elemental scans of pure PEO (right).

noted that the binding efficiencies of these nanofiber mats are much greater than that of a 93 μm solution-cast film of similar composition (0.44 mg/g chitosan) [17].

We have developed a model to predict Cr (VI) binding capacity of chitosan blend fibers [27] with known fiber diameter, % chitosan in blend solution, and chitosan % DDA. The model predicts that the binding capacity should vary by 30% over the range of diameters studied (88–131 nm) which is well within the standard deviation of the obtained results. It is observed that with increasing gsm for chitosan/PEO blend fibers (Fig. 5), a slight decrease in binding capacity is observed. The % chromium bound does not change with increasing fiber mat gsm (% chromium bound after 10 passes for 0.5 gsm web = 5.67%, 1 gsm web = 6.77% and 1.5 gsm web = 5.4%) which indicates that the binding efficiency of the fibers is constant irrespective of the basis weight of the mat. SEM images of dried HMW chitosan: PEO (90:10) blend nanofibrous filter after binding

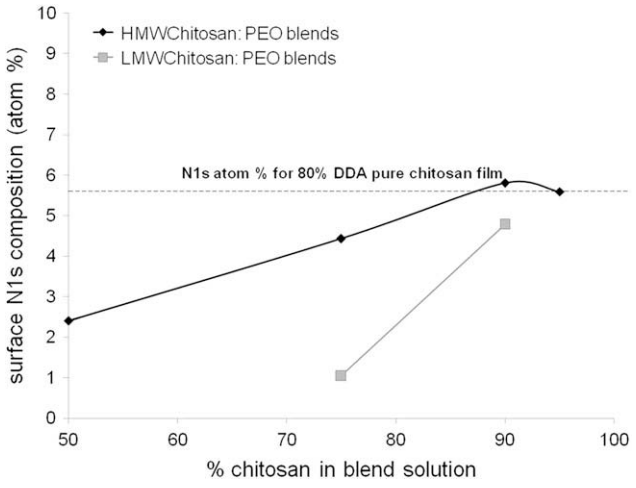

Fig. 3. Surface nitrogen (atom%) vs. chitosan wt% in blend solution.

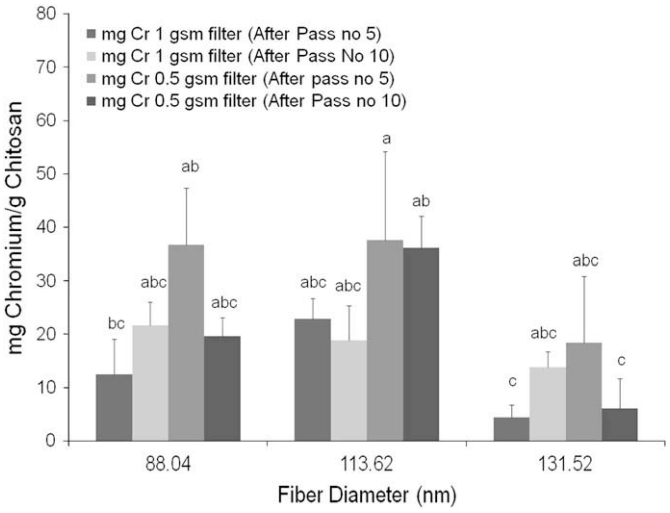

Fig. 5. Dynamic Cr(VI) binding capacity of 80% DDA 1.33 wt% HMWchitosan:PEO (90:10) blend fibers of varying fiber diameter and gsm(error bars represent standard deviation ($n = 3$), letters indicate significant difference at $p < 0.05$).

studies (Fig. 6) revealed a distinctly visible nanofibrous structure covered by a layer of polymer film. This film could be the redeposition of partially dissolved polymer which upon drying forms a film-like structure on top of the chitosan nanofibers. The XPS surface analysis of this film-like layer shows that the film has similar nitrogen content as pure chitosan film (atom% N of film layer = 4.83%, atom% N of pure chitosan film = 5.6%) which suggests that the film is rich in chitosan. It is hypothesized that during the binding experiments in aqueous medium, surface PEO dissolves in the water, while surface chitosan only partially dissolves or swells in the water. This swelling of chitosan could expose additional NH_3^+ sites for metal binding. In fact, our measured chromium binding efficiencies were 3 times higher than the maximum metal binding efficiencies predicted by our model [27]. Upon drying of this wet nanofibrous filter media, formation of a chitosan-rich polymer film would then appear on top of the electrospun fiber. This surface swelling effect may negate the expected effect of fiber diameter on binding properties as has been seen in Fig. 5. Although this swelling behavior may increase the initial binding capacity of the mats, the formation of a film-like layer during use will likely limit the extent to which these mats can be regenerated and reused.

3.3.2. *Effect of %DDA*

Fig. 7 shows the binding capacity of HMW chitosan: PEO (90:10) nanofibrous filter media with increasing % DDA. As has been seen in earlier static tests [17], binding capacity increased with increased % DDA even in the dynamic filtration studies. For the 67% and 70% DDA chitosan blend fibrous media there is no increase in binding between 5 and 10 passes as can be seen in the 80% DDA sample. The binding capacity of fibrous media fabricated with lower % DDA chitosan may saturate before or during pass #5 compared to the 80% DDA chitosan fibrous media.

Comparing metal binding results between the dynamic filtration tests obtained after 20 min of contact between fibers and metal solution and those discussed previously [17] wherein the contact time was 3 h, it can be seen that higher binding capacity per gram of chitosan fiber is observed in the dynamic filtration tests. This could be because of lower weight of fiber mats used in the dynamic tests (wt of filter mats used in dynamic studies is ~0.7–2.5 g, weight of mats used previously >3 g [17]). The thickness of the

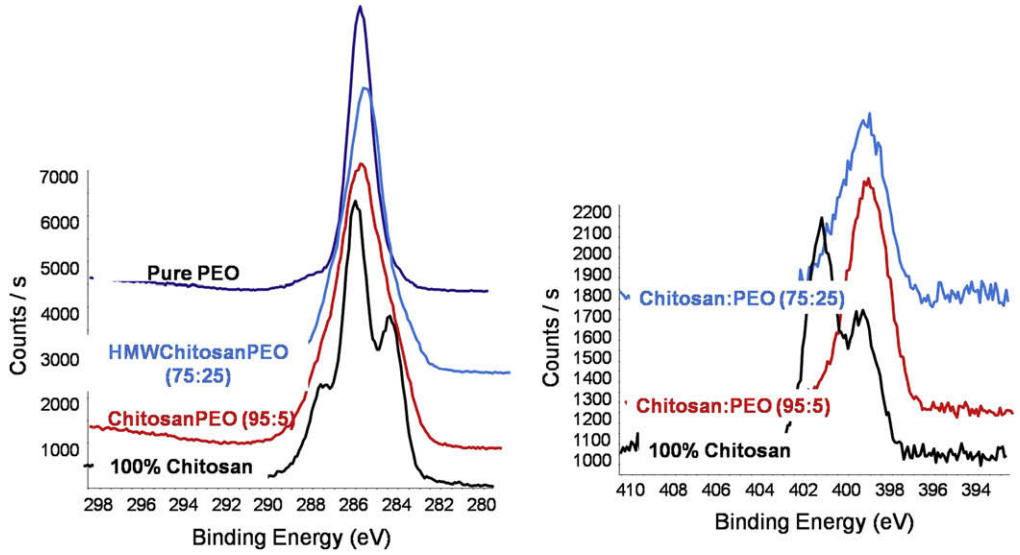

Fig. 4. C1s (left) and N1s (right) elemental scans of chitosan/PEO blend fibers with decreasing % chitosan in blend fiber.

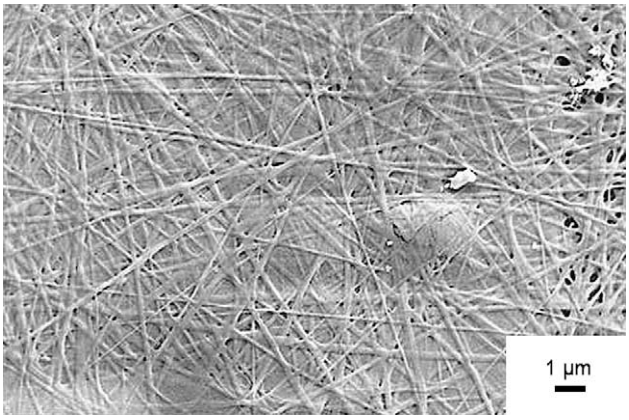

Fig. 6. SEM images of 1.33 wt% HMW chitosan:PEO (90:10) nanofibrous filter media after Cr (VI) binding.

nanofiber layer is ~3 microns. In the literature, it has been reported that the binding experiment reaches equilibrium after 12 h and after 20 min only 36% of available chromium has been bound by chitosan (i.e. 37.5% of maximum chromium ions that can be bound have been bound) [26]. Our studies show that after 20 min only ~7%–10% of chitosan is bound whereas the binding efficiency after 3 h testing is ~15%–30% [17]. The binding capacity after 20 min in dynamic filtration tests is approximately 40% of the maximum binding capacity (i.e. binding capacity after 3 h) which is similar to literature [26].

3.4. Anti-microbial properties of nanofibrous filter media

The anti-microbial properties of chitosan/PEO blend fibers were measured using the procedure outlined earlier. Chitosan fibers exhibit anti-microbial properties due to the positively charged NH_3^+ on the surface which can bind to the negatively charged components of the bacterial cell wall and inhibit the growth of the cell and eventually kill the microorganism. Effect of chitosan content in electrospun chitosan/PEO blend nanofibers, molecular weight of chitosan, and degree of deacetylation of chitosan were studied on anti-microbial performance of chitosan/PEO blend nanofibers. In anti-microbial studies, the reduction in microbial activity is normally reported on log basis. However, since all previous analysis has been based on weight of chitosan, we have also plotted data based on reduction in bacteria cfu (colony forming unit) divided by weight of the electrospun mat (Fig. 8). Increasing % PEO in blend fiber and decreasing molecular weight of chitosan leads to reduction in anti-microbial properties. We see a 2.5–3.0 log reduction indicating a bacteriostatic effect, this value is similar to ones reported for 35 μm thick films of chitosan:PEO blends with similar blend ratios and similar MW chitosan, but the mass of chitosan in films was up to 10 times higher than in the fibers [28]. The effect of molecular weight on anti-bacterial activity of chitosan is not fully understood. Some groups have suggested there is a threshold molecular weight ~220 kDa until which the anti-microbial activity increases with increasing chitosan molecular weight. However, upon exceeding this threshold molecular weight the anti-microbial activity decreases because it is believed the molecules pack more densely leading to increased inter and intra-molecular hydrogen and a decrease in the number of available protonated amine sites [29]. Fig. 9 shows a plot of effect of increasing chitosan % DDA for 1.33 wt% HMW chitosan:PEO (90:10) blend fibers. Although one would expect an increase in anti-microbial activity with increasing % DDA because of the increase of number of available protonated amine sites, results from Fig. 9 show the contrary. The slight decrease in anti-microbial activity with increasing % DDA could be because fibers formed at 80% DDA have larger fiber diameter (118 nm) compared to the fibers formed using 70% and 67% DDA (62 and 45 nm respectively). This increase in fiber diameter would lead to greater reduction in number of available protonated $-NH_3^+$ amine sites than would be increased by increasing % DDA. The number of available protonated $-NH_3^+$ sites at respective fiber diameters and % DDA for the 80% DDA and 70% DDA chitosan as calculated by our model are 2.15E+19 and 3.52E+19 which means the finer 70% DDA chitosan fibers have higher number of protonated amine sites which could result in better anti-microbial activity [27]. During all the anti-microbial tests, positive controls (no fibers present) as well as pure PEO electrospun mats were found to have 0 log reduction.

The anti-microbial properties of chitosan: PEO nanofiber membranes were studied using the dynamic filtration set-up. After 1 pass of 10^4 cfu/ml of *E. coli* K-12, less than 0.5 log reduction in bacteria was observed for all samples tested (varying fiber diameter, nanofiber gsm and chitosan DDA) for HMW chitosan:PEO

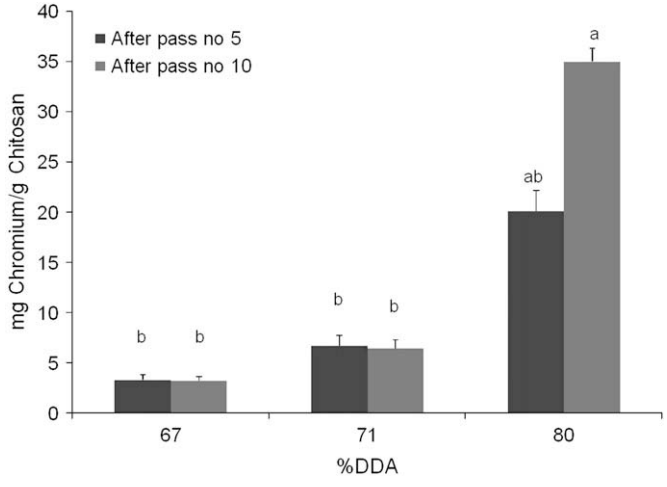

Fig. 7. Dynamic Cr(VI) binding capacity of HMWchitosan:PEO (90:10) blend fibers of varying chitosan % DDA (error bars represent standard deviation ($n = 3$), letters indicate significant difference at $p < 0.05$).

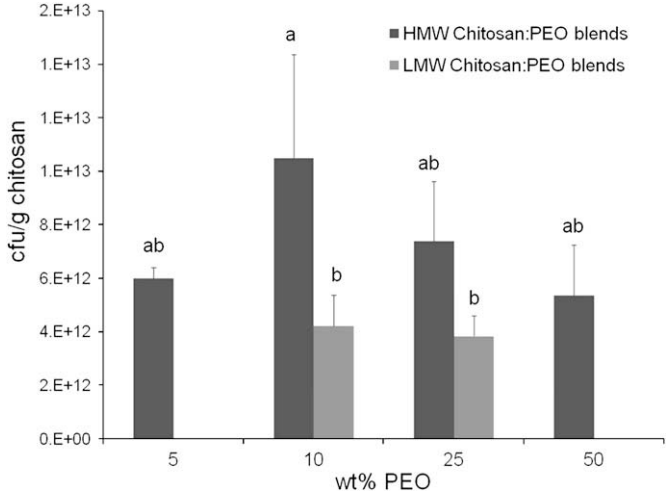

Fig. 8. Effect of % chitosan in blend fiber and molecular weight of chitosan in blend fiber on the # cfu/g chitosan in chitosan/PEO blend fibers of 80% DDA (HMW) (error bars represent standard deviation ($n = 3$), letters indicate significant difference at $p < 0.05$, $n = 3$).

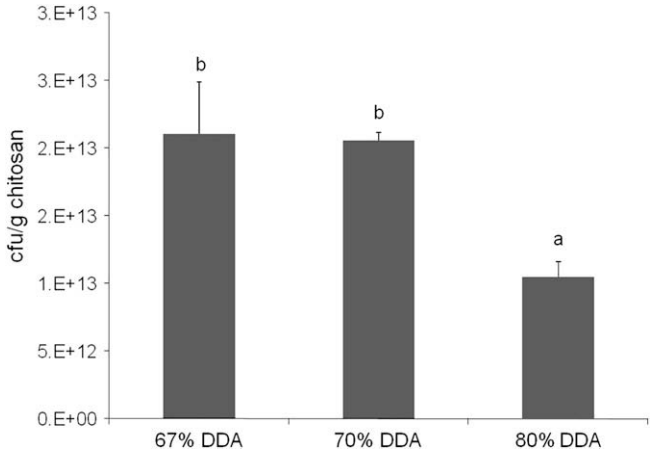

Fig. 9. Effect of chitosan % DDA on the of # cfu/g chitosan in chitosan/PEO (90:10) blend fibers (error bars represent standard deviation ($n = 3$), letters indicate significant difference at $p < 0.05$, $n = 3$).

(90:10) blend fibers after ~2 min of contact of fiber with bacterial solution. To understand the kinetics of the anti-microbial activity of chitosan, a time dependant test wherein bacterial survival after contact times between 2 min and 6 h were measured for 1 gsm 80% DDA HMW chitosan:PEO (90:10) blend fibers soaked in 10^7 cfu/ml bacteria solution. As seen in Fig. 10, there was <1 log reduction up to 2 h in bacteria and increased activity (>2 log reduction) only occurred after 4 h. Therefore, whatever reduction in bacteria was seen in the dynamic filtration test was probably due to the size effect of the nanofiber (which can trap the approximately 0.5 micron sized *E. coli* bacteria) and not any metabolic mechanism.

3.5. Physical filtration properties of chitosan nanofibrous filter media

The applicability of chitosan based nanofibrous filter media to effectively filter out heavy metal ions and micro-organism from pollutant water streams based on the polycationic nature of chitosan has been discussed so far.

The particle filtration efficiency of chitosan based nanofibrous filter media was characterized by passing 10 ml of 3 micron sized 200 ppm polystyrene beads through filter media using filtration

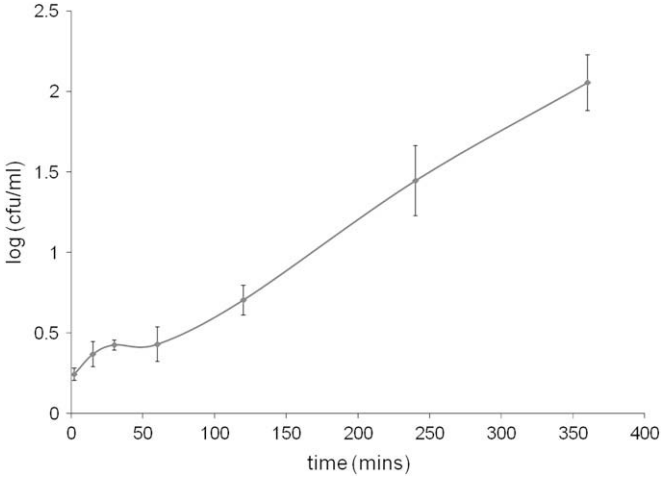

Fig. 10. Log reduction in *E. coli* test micro-organism after soaking 1 gsm HMW chitosan/PEO (90:10) nanofibrous filter media for different times in bacteria solution (right) (error bars represent standard deviation ($n = 3$)).

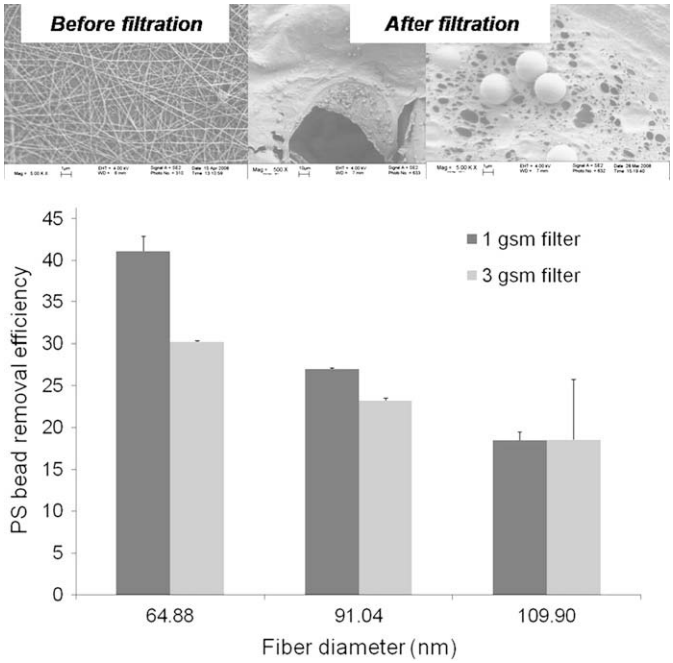

Fig. 11. SEM images of 1 gsm HMW chitosan:PEO nanofibrous filter media before and after passing 10 ml of 200 ppm 3 μm PS beads (top), PS bead removal efficiency of varying fiber diameter and fiber gsm HMW chitosan:PEO nanofibrous filter media (bottom).

set-up. Fig. 11 shows the filtration efficiency of 80% DDA HMW chitosan/PEO (90:10) blend nanofibrous filter media of varying fiber gsm and fiber diameter. With increasing fiber diameter, the PS bead filtration efficiency decreased. This is likely due to higher maximum pore size observed with increasing fiber diameter along with increase in air permeability (measured max. pore size of 1 gsm 65 nm diameter fiber = 1.95 μm, measured max. pore size of 1 gsm 110 nm diameter fiber = 2.5 μm). Fig. 11 also shows the SEM images of HMW chitosan/PEO (90:10) blend nanofibrous filter media before and after passing PS beads. It can be seen that the fiber mats appear to be torn after filtration. The mechanical integrity of the mat has been affected by the pressure exerted by the applied vacuum (~2 mm Hg) on the filter membrane during the

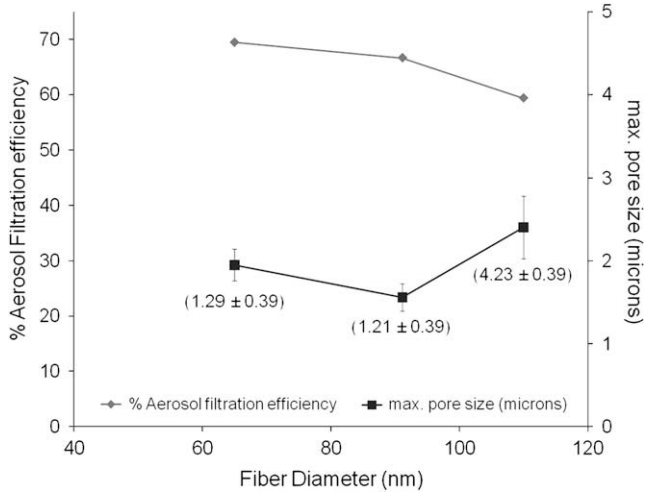

Fig. 12. Aerosol filtration efficiency and maximum pore size of 1 gsm HMW chitosan:PEO (90:10) nanofibrous filter media (numbers in parenthesis are the air permeability values in cfm for nanofiber mats at different fiber diameters, error bars represent standard deviation ($n = 3$)).

experiment. Therefore, a filtration experiment was also conducted without applying vacuum to the filter media for filtration and varying the fiber media gsm. A 1 gsm nanofibrous filter media of 92 nm fiber diameter and 1.562 microns maximum pore size achieved a 50% filtration efficiency and a similar 3 gsm nanofibrous filter media exhibited 70% filtration efficiency. Gopal et al. have reported high filtration efficiencies up to 92% for 1 micron sized PS bead particles [30] using a system which had better control over the pressure exerted on the nanofibrous membrane. However, our results obtained do attest to the fact that the chitosan based nanofibrous filter media can effectively filter out particulate media based on size as well as chemical nature of the contaminants.

To study the airborne particulate filtration efficiency based on the size of the nanofibers, the aerosol filtration efficiency (Fig. 12) of 1 gsm 80% DDA HMW chitosan: PEO (90:10) fibers of varying fiber diameters were measured. It can be seen that with increasing fiber diameter the filtration efficiency decreased because the maximum pore size and air permeability increased. These results show similar trend with those observed for other tested electrospun nanofiber media in literature [31,32]. The filtration efficiency values are similar to those obtained by Qin Wang et al. [33] (55%filtration efficiency against 0.6 μm NaCl aerosol particles using a 1 gsm 200 nm diameter and 1.76 μm maximum pore size electrospun poly(vinylalcohol) nanofibers). SEM images of the fiber sample before and after filtration showed no damage to the electrospun layer.

4. Conclusions

The work presented herewith demonstrates the applicability of chitosan based nanofibrous filter media to effectively filter out heavy metal ions, pathogenic micro-organisms, and contaminant particulate media from both air and water media. Chitosan based nanofibrous filter media offers the distinct advantage of using both size and surface chemistry of fibers to achieve desired filtration properties compared to nanofibrous filter media fabricated from other synthetic polymers.

Nanofibrous filter media using previously developed chitosan based electrospun nanofibers were successfully fabricated by electrospinning onto spunbonded PP non-woven substrates. XPS analysis of chitosan blend fibers show that with decreasing % chitosan in blend solution the surface nitrogen concentration decreases for chitosan/PEO blend solutions as expected. Dynamic metal binding efficiencies using as little 0.5 gsm of nanofibrous filter media showed promising results (binding capacity up to 35 mg chromium/g chitosan) for commercial applicability of these filters. The nanofibrous filter media however was unable to achieve desired anti-microbial effectiveness because of the slow reaction between the protonated amine in chitosan and negative components of the bacterial cell wall. However, after 6 h of contact time the chitosan blend fibers did show a 2–3 log reduction in *E. coli* cfu. Air and water filtration efficiencies of the nanofibrous filter media measured using aerosol and PS beads suspended in water respectively showed high efficiencies which correlated with the fibrous media size and shape. However the nanofibrous layer lacked mechanical strength to with stand pressure applied during the PS bead filtration which affected the results.

Filter media developed using an environmentally benign, naturally occurring biodegradable biopolymer chitosan offers unique advantages and has immense potential application for filtration purposes.

Acknowledgements

This research is funded by U.S. EPA Science To Achieve Results (STAR) Program Grant # GR832372.

References

[1] Kaur S, Gopal R, Ng WJ, Ramakrishna S, Matsuura T. MRS Bulletin 2008;33(1):21–6.
[2] Wang J, Kim SC, Pui DY. Journal of Aerosol Science 2008;39(4):323–34.
[3] Cauchie HM. Hydrobiologia 2002;470(1–3):63–96.
[4] Roberts GAF. Chitin chemistry. London: The MacMillan Press Ltd; 1992.
[5] Wu T, Zivanovic S, Draughon FA, Sams CE. Journal of Agricultural and Food Chemistry 2004;52(26):7905–10.
[6] Sorlier P, Denuziere A, Viton C, Domard A. Biomacromolecules 2001;2(3):765–72.
[7] Angelova NM, Rashkov I, Maximova V, Bogdanova S, Domard A. Journal of Bioactive and Compatible Polymers 1995;10(4):285–98.
[8] Helander IM, Nurmiaho-Lassila EL, Ahvenainen R, Rhoades J, Roller S. International Journal of Food Microbiology 2001;71(2–3):235–44.
[9] Lim SH, Hudson SM. Journal of Macromolecular Science—Polymer Reviews 2003;C43(2):223–69.
[10] Doshi J, Reneker DH. Journal of Electrostatics 1995;35(2–3):151–60.
[11] Podgorski A, Balazy A, Gradon L. Chemical Engineering Science 2006; 61(20):6804–15.
[12] Gibson P, Schreuder-Gibson H, Rivin D. Colloids and Surfaces A: Physicochemical and Engineering Aspects 2001;187-188:469–81.
[13] Ahn YC, Park SK, Kim GT, Hwang YJ, Lee CG, Shin HS, et al. Current Applied Physics 2006;6(6):1030–5.
[14] Schreuder-Gibson HL, Truong Q, Walker JE, Owens JR, Wander JD, Jones WE. MRS Bulletin 2003;28(8):574–8.
[15] Son WK, Youk JH, Park WH. Carbohydrate Polymers 2006;65(4):430–4.
[16] Shin GGC. AIChE Journal 2004;50(2):343–50.
[17] Desai K, Kit K, Li J, Zivanovic S. Biomacromolecules 2008;9(3):1000–6.
[18] Arof AK, Morni NM, Yarmo MA. Materials Science and Engineering B 1998; 55(1–2):130–3.
[19] Method 7600, 4 ed. NIOSH Manual of Analytical Methods (NMAM), National Institute of Occupational Safety and Health;1994.
[20] Swanson KMJ, Petran RL, Hanlin JH. Culture methods for enumeration of microorganisms. Washington, DC: American Public Health Association; 2001.
[21] Kriegel C, Weiss J, Kit K. Abstracts of Papers of the American Chemical Society; 2008. p. 042.
[22] Matienzo LJ, Winnacker SK. Macromolecular Materials and Engineering 2002;287(12):871–80.
[23] Chen ZJ, Lu XL, Chan CM, Mi YL. European Polymer Journal 2006;42(11):2914–20.
[24] Thomas HR, O'Malley JJ. Macromolecules 1979;12(2):323–9.
[25] Rjeb A, Letarte S, Tajounte L, El Idrissi MC, Adnot A, Roy D, et al. Journal of Electron Spectroscopy and Related Phenomena 2000;107(3):221–30.
[26] Udaybhaskar P, Iyengar L, Rao A. Journal of Applied Polymer Science 1990; 39(3):739–47.
[27] Desai K. Nanostructured chitosan membranes for filtration. PhD thesis, Department of Materials Science and Engineering, Knoxville: The University of Tennessee; 2008. pp. 167.
[28] Li J, Zivanovic S, Davidson M, Kit K. Abstracts of Papers of the American Chemical Society; 2007. p. 234.
[29] Shimojoh M, Masaki K, Kurita K, Fukushima K. Nippon Nogeikagaku Kaishi—Journal of the Japan Society for Bioscience Biotechnology and Agrochemistry 1996;70(7):787–92.
[30] Gopal R, Kaur S, Feng CY, Chan C, Ramakrishna S, Tabe S, et al. Journal of Membrane Science 2007;289(1–2):210–9.
[31] Yun KM, Hogan Jr CJ, Matsubayashi Y, Kawabe M, Iskandar F, Okuyama K. Chemical Engineering Science 2007;62(17):4751–9.
[32] Maze B, Vahedi Tafreshi H, Wang Q, Pourdeyhimi B. Journal of Aerosol Science 2007;38(5):550–71.
[33] Qin X-H, Wang S-Y. Journal of Applied Polymer Science 2006;102(2):1285–90.